Journal of Chromatography, 185 (1979) 261–271

CHROM. 12,146

STERIC FIELD-FLOW FRACTIONATION AS A TOOL FOR THE SIZE CHARACTERIZATION OF CHROMATOGRAPHIC SUPPORTS

J. CALVIN GIDDINGS, MARCUS N. MYERS, KARIN D. CALDWELL and JOSEPH W. PAV
Department of Chemistry, University of Utah, Salt Lake City, Utah 84112 (U.S.A.)

SUMMARY

Steric field-flow fractionation is described and its application to the determination of the mean size and size distribution of chromatographic supports is suggested. After measuring systematic departures from theoretical retention values, a calibration curve is constructed using microporous silica beads whose mean diameters (4.4, 6.4, 12.1 μm) are accurately determined by electron microscopy. Other spherical chromatographic support materials are shown to cluster around the calibration curve. Fractograms (elution curves) are then shown for 15 spherical supports and six irregular supports. It is shown that the fractograms yield information on mean particle diameters, dispersion, and skewness, the latter possibly reflecting high concentrations of fine and coarse particles. Some limitations and future needs in the application of the method are noted.

INTRODUCTION

Steric field-flow fractionation (FFF) is a relatively new technique designed for the separation of particles according to their size. We suggest that this technique may complement existing sizing methods by providing information about the size distribution of particulate systems via a quick and simple procedure. In a recent publication, separation was demonstrated and it was suggested that particles in the range 1–100 μm could readily be fractionated[1]. The possibility of extending the steric concept to a continuous system has also been explored[2].

The purpose of this report is to study the basic parameters of steric FFF system as part of an effort to improve resolution, accuracy, and speed. A practical application of this system is also provided through the testing of various chromatographic support materials. The support materials used for high-performance liquid chromatography are ideal for this application because of their small size, high density and general sphericity.

FFF is normally utilized in the study of macromolecules and particles in the sub-micron size range. In this technique, a field is applied in a direction perpendicular to the flow channel, forcing each solute into a thin layer of unique effective thickness[3,4]. The solute zone or layer moves downstream at a velocity determined by its thickness and thus by its position in the laminar flow of the solvent. When FFF is

used with high fields and large particles, the particles are forced against the wall of the channel by the field and the mean particle displacement away from the wall due to Brownian motion becomes much less than the particle radius[1]. The rate of motion of the particles in the flow stream is therefore determined only by the size of the particles.

THEORETICAL

The retention ratio R (channel volume/particle retention volume) is given approximately by

$$R = \frac{6a}{w} + \frac{6l}{w} \tag{1}$$

where a is the particle radius, w is the thickness of the channel, and l is the mean Brownian displacement from the wall. When l is small, as in the case of high relative fields, the retention ratio reduces to the steric term alone

$$R = \frac{6a}{w} \tag{2}$$

In this limit, steric FFF is fully operational and retention is determined only by the particle radius a.

Any influences that would take the particles away from the wall would necessarily affect the R value. Therefore the channel surface should be flat and smooth and when a gravitational field is used the particles should be denser (or less dense) than the carrier. The particles, of course, must not be prone to adhesion.

To ensure that the particles reach the surface of the flow channel after injection, the system must be allowed time to relax: the flow must be stopped so the particles can settle. The relaxation time necessary for complete settling under the influence of gravity alone can be determined by the expression

$$\tau = w/U \tag{3}$$

where settling velocity U is expressed by

$$U = \frac{M'g}{6\pi\eta a} = \frac{2a^2\Delta\varrho g}{9\eta} \tag{4}$$

where M' is the effective particle mass (real mass minus buoyant mass), η the carrier viscosity, g the acceleration due to gravity and $\Delta\varrho$ the density difference between particle and carrier. By way of example, 4.42 μm particles with $\varrho = 1.5$ g/ml (approximating our standard microporous silica beads) require $\tau = 24$ sec to settle 0.127 mm (our channel thickness w) through an aqueous solution of $\varrho = 1.0$ g/ml and $\eta = 0.010$ P.

The steric FFF method is expected to work best (and is certainly understood best) for spherical particles. However, irregular particles would be displaced in the

same general way, but the mechanism of motion would be more complex than that for their spherical counterparts[1].

The retention volume in steric FFF can be defined by the expression

$$V_r = V^0/R \tag{5}$$

When eqn. 2 is used for R, eqn. 5 assumes the approximate form

$$(V_r/V^0) = w/6a \tag{6}$$

Eqn. 6 indicates that large particles will be carried down the channel more rapidly than small particles. Quantitatively, the retention volume is expected to be inversely related to particle size, contrary to the elution order normally encountered in FFF. This report will examine the inverse relationship and demonstrate the utility of steric FFF in size characterization.

EXPERIMENTAL

A steric FFF column was made by sandwiching a 0.127 mm (0.005 in.) mylar spacer between 12.7 mm (0.5 in.) thick glass plates. The column was then held together by two Plexiglas clamping bars. Each bar was 6.35 mm (2.5 in.) thick, which ensured an even pressure on the glass plates when tightly clamped. Clamping was achieved with 72 bolts placed along the edges of the column, each torqued to 35 inch-pounds. The resulting flow channel had the dimensions of 0.127 mm by 10 mm by 1.773 m and a volume of 2.25 ml. The principal carrier liquid was 0.01 M ammonia in distilled water. The carrier was introduced into the channel by a Chromatronix Cheminert (Model CMP-IV) metering pump at a flow-rate of 59 ml/h. An LDC UV-detector (Cat. No. 1285) with a 10-μl flow-through cell operating at a wavelength of 254 nm was used for detection. All work was done at laboratory temperature, 25° ± 1°.

The sample particles used for column calibration were three sizes of porous silica microspheres, provided by Dr. Jack Kirkland of E. I. duPont deNemours & Co., (Wilmington, Del., U.S.A.). The calibration particle diameters (nominal values 5.6, 7.5 and 10–14 μm) were checked using microscopic techniques, primarily by comparing photomicrographs of the particles with the photomicrograph of a microscopic scale from Leitz (Wetzlar, G.F.R.). (The same technique was applied to the chromatographic supports using a minimum of 30 particles per support.) Magnifications of 400× and 1000× on a phase contrast microscope with a green filter were utilized for most work. For the calibration particles more precise measurements were made using a Phillips transmission electron microscope (Model EM 201) at a magnification of 2000×. The particles appeared as clear images with sharp boundaries on a black background in the photographic film from the electron microscope. Sizes were obtained by comparison of densitometer scans of the film relative to scans of a grid containing 1134 lines/mm. The densitometer scans provided a sharp deflection as the particle boundary on the film passed through the detector beam (Fig. 1). A minimum of 15 particles were used to determine particle sizes. Reproducibility for an individual particle diameter was good (*e.g.*, 6.72 ± 0.12

μm for three repetitions) and a study of the densitometer measurement using different diameters of the same particle indicated that the particles were indeed spherical (6.86 $\pm$ 0.21 μm for six different choices of diameter).

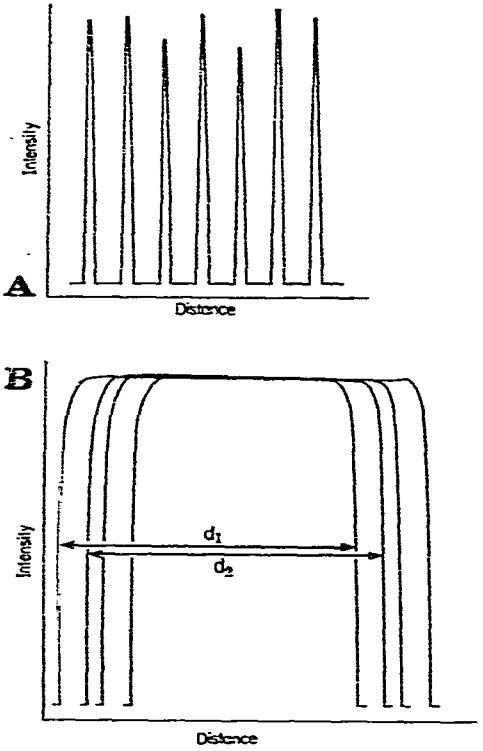

Fig. 1. Densitometer plots of film showing (a) grid containing 1134 lines/mm, and (b) sample spheres with distance measured by lengths d_1, d_2, etc.

Following calibration, steric FFF was applied to the study of chromatographic supports. Samples were provided by Rainin Instr. (Woburn, Mass., U.S.A.), Johns-Manville (Denver, Colo., U.S.A.). Dr. Csaba Horváth, and Dr. Barry Karger. Support materials studied were restricted to those which were more dense than the solvent. Less dense supports could conceivably be fractionated also. All samples were injected by syringe using 10–20 μl of injected volume.

RESULTS AND DISCUSSION

The electron microscope–densitometer technique illustrated in Fig. 1 yielded the following mean diameters for the porous silica calibration beads: 4.42, 6.40, and 12.08 μm for the nominal 5.6, 7.5, and 10–14 μm beads, respectively.

A study of injection techniques was made by observing the peak eluted after injecting a solution of malachite green under various conditions. Injection parameters included the depth of needle insertion, direction of needle opening, and length of

time of needle insertion. The study failed to turn up any significant differences due to changes in the above parameters.

The effect of a variable relaxation time on retention is shown in Fig. 2. Samples of the smallest porous silica beads (diameter $d = 4.42$ μm) were injected at a flow-rate of 59 ml/h. Immediately after injection, the flow was stopped and the sample was allowed to settle (relax) toward the bottom wall of the flow channel. The rate at which particles settle, as shown by eqns. 3 and 4, is dependent on their sizes and the density difference in relation to the solvent. The small beads used in this experiment ($d = 4.42$ μm) were calculated to require 24 sec for relaxation, as specified in the example following eqn. 4. Theoretically, then, R should not change for any extension in the stoppage of flow beyond 24 sec. Fig. 2 shows that the change in retention due to variable stop-flow times continues up to *ca.* 3 min, although the effect is small beyond 2 min. The delay of *ca.* 2 min before the onset of steady retention is far longer than the theoretical value of 24 sec, calculated for pure water. There will be a slight perturbation in the ϱ and η terms of eqn. 4 because of the use of a 0.01 M ammonia solution, but the perturbation appears to be <0.1%, a negligible value. The discrepancy in theoretical and experimental relaxation times is most likely due to the presence of entrapped air in the micropores of the beads, leading to reduced bead densities that may in some cases approach the density of the solution.

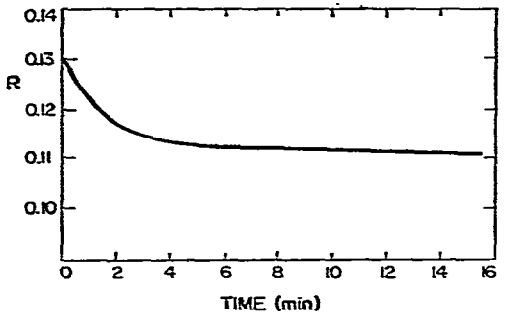

Fig. 2. Effect of stop-flow time on the retention (R) of the smallest (d *ca.* 5 μm) porous silica beads.

In the first paper on steric FFF[1], the possible influence of flow velocity on retention was discussed. It was suggested that as long as viscous forces dragging and rolling the particles along exceed the gravitational forces pulling the particles to the wall, steric FFF would be optimal. This argument would suggest that the higher velocities would be an advantage for steric FFF, completely aside from the obvious gain in analysis speed. Furthermore, there should be no effect of velocity on the retention ratio under these high-flow conditions. Our present experimental evidence, however, shows that the retention ratio R increases as the flow-rate increases (Fig. 3). However, the R values start much below the theoretical value and surpass this value only at very high velocities.

By extending our studies to other solvent systems, the effect of viscosity on the flow velocity *vs.* retention ratio dependence is observed. The two additional solvents chosen, methanol and isobutanol, are both less dense than water with values of

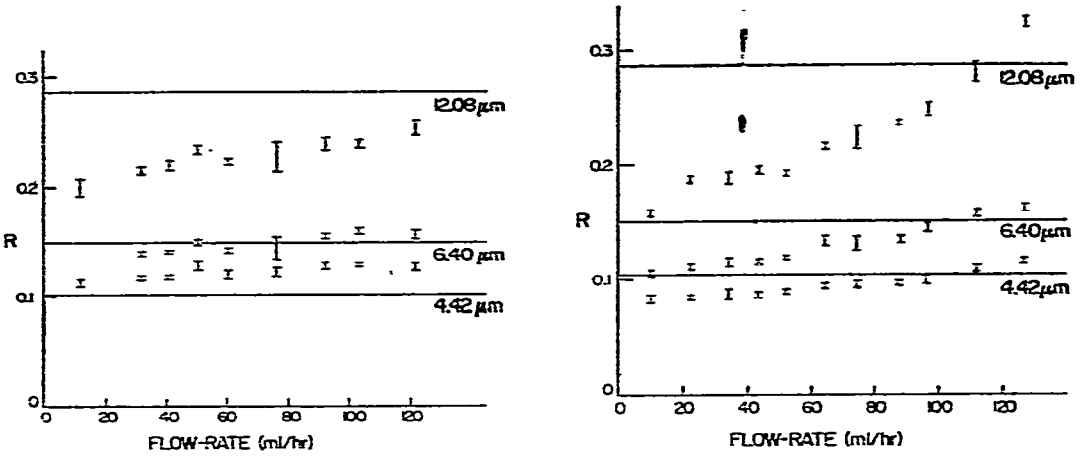

Fig. 3. Retention ratio R *vs.* flow-rate for the three sizes of calibration beads in 0.01 M ammonia. Straight lines are the theoretical values from eqn. 2. Three runs were made for each experimental value.

Fig. 4. Retention ratio *vs.* flow-rate for the three sizes of calibration beads in methanol. Three runs per experimental value.

0.79 and 0.81 g/ml, respectively, at 20°. At this temperature, the viscosity of methanol is 0.597 cP and that of isobutanol 2.948 cP. In Fig. 4 the results are plotted for methanol, a significantly less viscous solvent than 0.01 M ammonia. The figure shows that the theoretical limit for R is exceeded only at high velocities for the intermediate size particle (as in the ammonia system), while R remains entirely below the theoretical value for the large particles and entirely above the limit for small spheres. The more viscous solvent, isobutanol, gives results similar to the aqueous system for the small and intermediate size particles, but not for the large beads, as shown in Fig. 5.

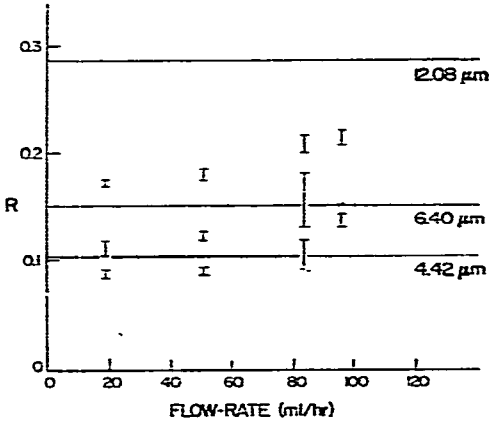

Fig. 5. Retention ratio *vs.* flow-rate for the three sizes of calibration beads in isobutanol. Three runs per experimental value.

The reason for the unexpected experimental trends in R *vs.* flow-rate curves is unknown. The studies using methanol and butanol solvents fail to cast a decisive light on the question. Additional studies are needed to resolve the matter.

The retention ratio provides only a partial characterization of the system. Zone broadening is another important factor. Zone broadening can be expressed as the number of theoretical plates, N. However, any measure of N reflects sample polydispersity as well as column behavior. Nonetheless, trends in N should reflect column processes because the polydispersity contribution is expected to be relatively constant with respect to changes in flow-rate. These trends are shown in Fig. 6 for the aqueous ammonia solution. The decrease in N as velocity increases is unexpected[1]. However, from an empirical point of view, several hundred plates in a highly selective system like steric FFF provide good resolution with respect to most particle mixtures, which tend to be rather non-uniform. Therefore, we arbitrarily chose a flow-rate of 59 ml/h, which provides reasonable resolution and, at the same time, relatively high speed.

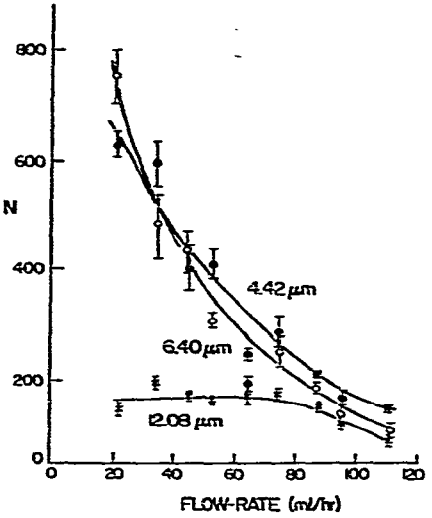

Fig. 6. Effect of flow-rate on the number of theoretical plates (N) for calibration beads of the mean diameters indicated.

The number of theoretical plates was more difficult to measure in other solvents. The fractograms produced when using methanol and isobutanol were of poor resolution and reproducibility.

All samples of spherical chromatographic support particles were sized using the microscopic technique noted earlier. The observed sizes were compared to the reported values. Table I shows that the two values generally agree to within *ca.* 20% for the various supports.

Table I shows that the microporous silica beads provided by Kirkland have the best uniformity of size. This uniformity explains why we have used these beads as calibration standards for steric FFF. For calibration, repetitive steric FFF runs of these three particles were made and retention volumes were calculated based on the position of emergence of the peak center. Mean particle diameters were assessed

TABLE I

COMPARISON OF PARTICLE DIAMETERS BY DIFFERENT APPROACHES

Commercial supports	*Particle diameter (μm)*		
	Reported	*Microscopic*	*Steric FFF**
Spherical			
(A) duPont silica beads	5.6 ± 0.9	4.42 ± 0.26**	
(B) duPont silica beads	7.45 ± 0.85	6.40 ± 0.29**	
(C) duPont silica beads	10–14	12.08 ± 0.89**	
(D) Nucleosil 71201	5	4.7 ± 0.7	5.0 ± 0.7
(E) Spherisorb 2.214	5	5.8 ± 1.1	6.0 ± 0.6
(F) Hypersil GA364	5	5.8 ± 0.8	5.6 ± 1.0
(G) Hypersil GA279	4.5	5.6 ± 0.8	6.2 ± 1.0
(H) Spherisorb Alumina AlOY	10	10.0 ± 2.2	8.5 ± 1.7
(I) Sephasorb		16.6 ± 3.8	20.8 ± 6.5
(J) Aminex A5		11.8 ± 1.1	16.9 ± 6.7
(K) Aminex A6	17.5 ± 2	16.2 ± 1.1	16.4 ± 1.6
(L) LiChrospher SI 100	5	4.7 ± 0.7	8.1 ± 2.1
(M) Silica–polar nitrile phase	10	8.3 ± 0.7	6.1 ± 2.5
(N) Silica–cation exchanger	10	8.3 ± 1.1	8.3 ± 3.0
(O) Silica–anion exchanger	5	5.0 ± 0.7	67 ± 54
Irregular			
(P) Partisil 5A312	6		13.3
(Q) Alumina	3		11.9
(R) Silica gel	20		34.5
(S) Aluminum oxide	5		20.8
(T) LC-6	5		15.4
(U) LC-6	10		34.5

* Sizes determined using duPont calibration beads.
** Determined by electron microscope–densitometer.

by the electron microscope–densitometer technique, as noted earlier. A least-squares regression was employed to determine the calibrated retention volume–particle size plot shown in Fig. 7.

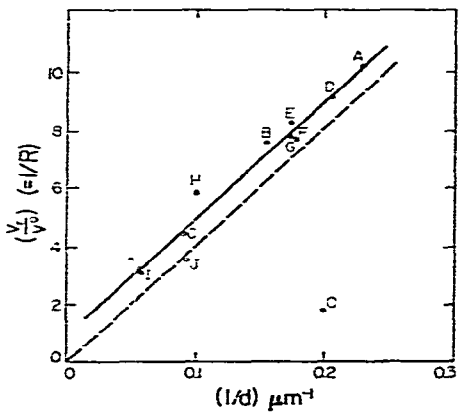

Fig. 7. Correlation of retention volume V_r with particle diameter d using calibration beads (A, B, C). The dashed line through the origin is from eqn. 6. The other data are keyed by letters to the support materials listed in Table I.

The retention volumes of most of the spherical support materials are also plotted against reciprocal diameters (measured microscopically) in Fig. 7. On the whole the points cluster fairly near the line. The only serious departure is due to support O, which will be discussed subsequently. It should be noted that the mean sizes determined for steric FFF are calculated using the position of the peak maximum. This procedure is acceptable for samples with a fairly narrow, symmetrical distribution.

The theoretical retention volume curve, obtained from eqn. 6, is shown as the dashed line in Fig. 7. Although the theoretical curve is fairly close to the calibration curve, and exhibits about the same slope, the calibration curve is generally in better accord with the experimental data.

Figs. 8 and 9 show some of the fractograms for spherical supports. The distribution of support particle sizes is reflected in the width and shape of the curve, and is subject to rapid interpretation. As an example, we confirm immediately by inspection that three microporous silica calibration beads (shaded peaks in Fig. 8), along with Aminex A6, have unusually narrow distributions. These results are confirmed by the microscopic results of Table I. We also see the suggestion of a high content of smaller-than-average particles, or "fines", in curves such as H and I. A small fraction of coarse material is suggested for curves M and N. Thus we can assume, with some reservations noted below, that we have the beginning of a quick and, both numerically and visually, direct method for acquiring mean size and size distribution data for chromatographic supports and other particulate systems.

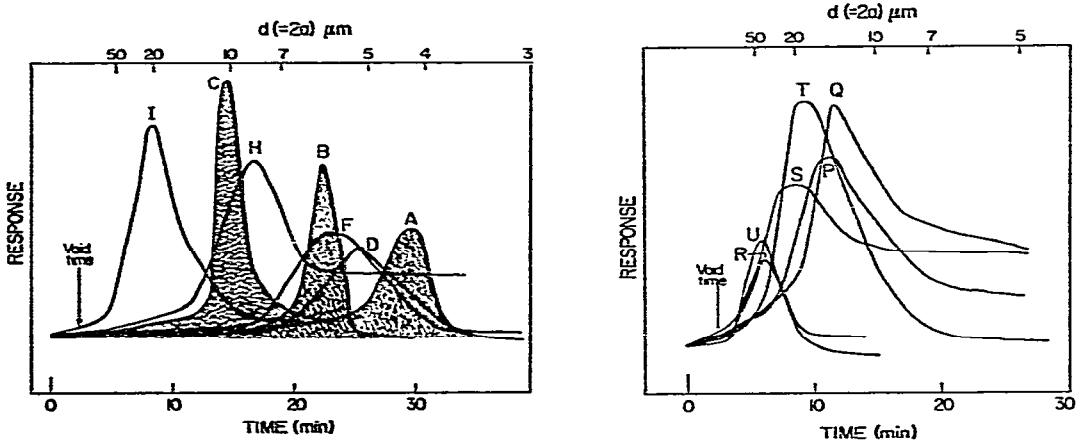

Fig. 8. Fractograms of spherical support materials in 0.01 *M* ammonia. Calibration particles are shaded. Letters refer to the support materials in Table I.

Fig. 9. Fractograms of spherical support materials in 0.01 *M* ammonia. Letters refer to the support materials in Table I.

A rough expression for size polydispersity can be gained by measuring peak broadening. The standard deviation in particle diameter, σ_d, can be approximately obtained as one-half the peak width at $e^{-\frac{1}{2}}$ (= 0.6065) of the peak height using the d scale. These values are presented along with the "mean" diameters in Table I.

σ_d values are generally larger than the σ values obtained microscopically (σ_M). This is expected because of band broadening in the column and extra-column effects. The divergence is not large and could probably be reduced further by improved experimental techniques.

In certain cases the steric FFF system may yield diameter values that differ markedly from the actual value. Particle–particle adhesion would contribute to peak shifts and peak broadening. (Aggregation will also disturb many microscopic measurements.) For example, the silica anion exchanger (O) (with a bonded dimethylamino group) has a microscopic diameter of 5.09 μm, but steric FFF indicates a diameter of 67 μm. Apparently, in the basic ammonia solution, this anion exchanger has a tendency to aggregate. It is likely that changing to an acidic solution would reduce the aggregation, but acidification was not tried. The LiChrospher sample (L) gives abnormal results as well. A close examination of its fractogram shows a skewed peak suggesting a larger-than-expected diameter, but not large enough to explain the almost two-fold increase found.

The results obtained for irregular particles, shown in Fig. 10, require special consideration. In every case, the size determined by steric FFF is much greater than the reported size (Table I). It was originally suggested that the effective diameter for irregular particles would be the distance along their longest axis[1]. This suggestion is in accord with the results of Table I, but more precisely defined sample particles must be studied before any quantitative explanation of the results of Fig. 10 is possible. Since steric FFF does roughly reflect the relative order of size for irregular particles, the method may have a useful future for irregular particle analysis.

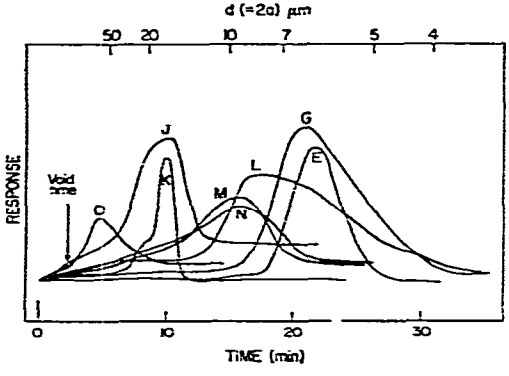

Fig. 10. Fractograms of irregular support materials in 0.01 *M* ammonia. Letters refer to the support materials in Table I.

CONCLUSIONS

The results presented in this paper show clearly that important size and size distribution information can be obtained for chromatographic supports and similar particulate systems. We have noted some of the limitations of this method which future investigators should carefully note.

The development of the calibration curve as we report here should be planned for each new steric FFF instrument put into use. While the calibration curve

appears to work adequately here, there is no assurance that it would work in all cases, particularly with particles having widely varying densities. This needs to be determined in individual cases.

Ultimately we hope to avoid the necessity of using a calibration curve: we would like to replace calibration by a simple theoretical expression such as eqn. 6. However, the anomalous deviations from theory apparent in Figs. 3–6 show that we are not yet ready to abandon empirical calibrations. One of the goals of future research is to obtain a better understanding of displacement processes and fractionation in steric FFF so that particle size distribution curves can be rather directly obtained. Another goal, of course, is the development of columns of higher efficiency and higher speed so that both accuracy and convenience are improved.

Finally, we should add that the use of the standard LC detector and UV detection cell for sample detection works well, but should be interpreted carefully for exact results. The bulk of the detector signal probably emanates from reflection and refraction at the glass–solution interface. The magnitude of this signal probably represents bead surface area more accurately than it does bead mass. The average fineness of pores in a support particle would also affect the attenuation of the beam. More work needs to be done in this area to obtain true mass distribution curves.

ACKNOWLEDGEMENT

This research was supported by National Science Foundation Grant No. CHE 76-20870 and by National Institutes of Health Biomedical Research Support Grant No. RR 07092.

REFERENCES

1 J. C. Giddings and M. N. Myers, *Separ. Sci. Technol.*, 13 (1978) 637.
2 M. N. Myers and J. C. Giddings, *Powder Technol.*, 23 (1979) 15.
3 J. C. Giddings, *J. Chem. Educ.*, 50 (1973) 667.
4 E. Grushka, K. D. Caldwell, M. N. Myers and J. C. Giddings, *Separ. Purif. Methods*, 2 (1974) 127.
5 J. C. Giddings, *Separ. Sci. Technol.*, 13 (1978) 241.